AIP | Proceedings

Photon assisted current in molecular nanojunctions with novel types of contacts

Boris D. Fainberg

Citation: AIP Conference Proceedings **1590**, 10 (2014); doi: 10.1063/1.4870189
View online: http://dx.doi.org/10.1063/1.4870189
View Table of Contents: http://scitation.aip.org/content/aip/proceeding/aipcp/1590?ver=pdfcov
Published by the AIP Publishing

Photon Assisted Current in Molecular Nanojunctions with Novel Types of Contacts

Boris D. Fainberg

Faculty of Science, Holon Institute of Technology, 58102 Holon, Israel
School of Chemistry, Tel-Aviv University, 69978 Tel-Aviv, Israel

Abstract. We propose new approaches to coherent control of transport via molecular junctions, which bypasses several of the hurdles to experimental realization of optically manipulated nanoelectronics noted in the previous literature. The first method is based on the application of intrinsic semiconductor contacts and optical frequencies below the semiconductor bandgap. Our analytical theory predicts a new phenomenon, referred to as coherent destruction of induced tunnelling, which extends the phenomenon of coherent destruction of tunnelling frequently discussed in the previous literature. We also propose to use graphene electrodes as a platform for effective photon assisted tunneling through molecular conduction nanojunctions. We predict dramatic increasing currents evaluated at side-band energies $\sim n\hbar\omega$ (n is a whole number) related to the modification of graphene gapless spectrum under the action of external electromagnetic field of frequency ω. Our results illustrate the potential of semiconductor and graphene contacts in coherent control of photocurrent.

Keywords: Molecular conduction nanojunctions, dressed states, semiconducting and graphene electrodes
PACS: 73.23.-b, 73.63.Rt, 78.67.Wj, 42.50.Hz

INTRODUCTION

The field of molecular-scale electronics has been rapidly advancing over the past two decades, both in terms of experimental and numerical technology and in terms of the discovery of new physical phenomena and realization of new applications (for recent reviews please see Refs.[1, 2]). In particular, the optical response of nanoscale molecular junctions has been the topic of growing experimental and theoretical interest in recent years [3, 4, 5, 6], fueled in part by the rapid advance of the experimental technology and in part by the premise for long range applications in optoelectronics. The ultimate goal of controlling electric transport with coherent light, however, has proven challenging to realize in the laboratory. One difficulty that has been noted in the previous literature is substrate mediated processes. Light shine on a molecular system in contact with a metal substrate is adsorbed by the substrate, rather than by a molecular bond or the molecule–surface bond in the vast majority of cases, leading to the excitation of hot carriers. The latter may interact with the molecule and lead to interesting dynamics, but in the process coherence is lost. Other competing processes include heating of the electrodes (one of which often consists of an STM tip) and undesired energy transfer events.

Reference [4] proposes the use of semiconducting electrodes and sub-bandgap frequencies to circumvent undesired substrate-mediated and heating processes. Here, an ultrafast, nanoscale molecular switch is introduced, consisting of a conjugated organic molecule adsorbed onto a semiconducting surface and placed near a scanning tunneling microscope tip. A low-frequency, polarized laser field is used to switch the system by orienting the molecule with the field polarization axis, enabling conductance. Semiconducting electrodes have been used in the experimental literature in the context of a single-quantum-dot photodiode that may be considered as a quantum dot-based junction [7, 8]. In addition to introducing a new opportunity for coherent control of transport via junctions, semiconductor-based molecular electronics offer potentially several other attractive properties. From a chemical perspective, organic molecules typically form much stronger bonds with semiconducting surfaces, such as doped silicon, than with metals. From a technological perspective, the addition of molecular function to the already established silicon-based technology is vastly more viable than replacing silicon by metal-based electronics.

In the first part of the work we propose and explore theoretically a new approach to coherent control of electric transport via semiconducting junctions, which is similar to the concept introduced in Ref. [4] in capitalizing on the use of sub-bandgap frequencies, but is complementary in application. Our approach is based on the excitation of dressed states of the junction Hamiltonian that can be frequency-tuned to tunnel selectively into either the left or the right contacts, thus generating unidirectional current whose temporal characteristics are controlled by the light pulse.

Furthermore, a way of the control of the current through molecular conduction nanojunctions is the well-

Electronic, Photonic, Plasmonic, Phononic and Magnetic Properties of Nanomaterials
AIP Conf. Proc. 1590, 10-19 (2014); doi: 10.1063/1.4870189

known photon-assisted tunneling (PAT) [9, 1] that was studied already in the early 1960's experimentally by Dayem and Martin [10] and theoretically by Tien and Gordon using a simple theory which captures already the main physics of PAT [11]. The main idea is that an external field periodic in time with frequency ω can induce inelastic tunneling events when the electrons exchange energy quanta ω with the external field. PAT may be related either to the potential difference modulation between the contacts of the nanojunction when electric field is parallel to the axis of a junction [11, 9, 5], or to the electromagnetic (EM) excitation of electrons in the metallic contacts when electric field is parallel to the film surface of contacts [11]. According to the Tien-Gordon model [11, 9, 5] for monochromatic external fields that set up a potential difference $V(t) = V_0 \cos\omega t$, the rectified dc currents through ac-driven molecular junctions are determined as [9, 5]

$$I_{TG} = \sum_{n=-\infty}^{\infty} J_n^2\left(\frac{eV_0}{\hbar\omega}\right) I_{dc}^0(eV_0 + n\hbar\omega) = \sum_{n=-\infty}^{\infty} I_n \qquad (1)$$

where the current in the driven system is expressed by a sum over contributions of the current $I_{dc}^0(eV_0 + n\hbar\omega)$ in the undriven case but evaluated at side-band energies $eV_0 + n\hbar\omega$ shifted by integer multiples of the photon quantum and weighted with squares of Bessel functions. A formula similar to Eq.(1) can be obtained also for EM excitation of electrons in the metallic contacts [11]. Note that the partial currents I_n contain contributions from $\pm n$. The term $J_n(\frac{eV_0}{\hbar\omega})$ denotes the n-th-order Bessel function of the first kind. The photon absorption ($n > 0$) and emission ($n < 0$) processes can be viewed as creating effective electron densities at energies $eV_0 \pm n\hbar\omega$ with probability $J_n^2(\frac{eV_0}{\hbar\omega})$. These probabilities strongly diminish with number n when $eV_0 \leq \hbar\omega$ that severely sidelines the control of the current for not strong EM fields ($< 10^6\ V/cm$ [1]).

In the last time graphene, a single layer of graphite, with unusual two-dimensional Dirac-like electronic excitations, has attracted considerable attention due to its exceptional electronic properties (ballistic in-plane electron transport etc.) [12, 13]. Quite recently they have shown interest to a new kind of graphene-molecule-graphene (GMG) junctions that may exhibit unique physical properties, including a large conductance (achieving 0.38 conductance quantum) etc. [14]. The junction consists of a conjugated molecule connecting two parallel graphene sheets. In this relation it would be interesting to investigate PAT in such a junction to control the current through it. The PAT in GMG junctions under EM excitation of electrons and holes in the graphene contacts may be rather different from that for usual metallic contacts. It was shown that the massless energy spectrum of electrons and holes in graphene led to the strongly non-linear EM response of this system [15]. Sure, the strongly non-linear EM response should also lead to a slow falling down currents evaluated at side-band energies $\sim n\hbar\omega$ (see Eq.(1)) with harmonics index n in comparison to nanojunctions with metallic (or semiconductor [16]) leads (see below). This makes controlling charge transfer essentially more effective than that for molecular nanojunctions with metallic contacts. Additional factors that may enhance currents evaluated at side-band energies $\sim n\hbar\omega$ in nanojunctions with graphene electrodes are linear dependence of the density of states on energy in graphene [12], and the gapless spectrum of graphene that can change under the action of external EM field (see below).

In the second part of the work we propose and explore theoretically a new approach to coherent control of electric transport via molecular junctions, using either both graphene electrodes or one graphene and another one - a metal electrode (that may be an STM tip). Our approach is based on the excitation of dressed states of the doped graphene electrode with electric field that is parallel to its surface, having used unique properties of graphene mentioned above.

PHOTON ASSISTED CURRENT IN MOLECULAR NANOJUNCTIONS WITH SEMICONDUCTOR CONTACTS [16, 17]

We consider a molecular junction consisting of a molecular moiety that possess a permanent dipole moment **D** and is in contact with two intrinsically semiconducting electrodes. The use of SC contacts circumvents energy transfer from the bridge to the contacts [8], a complicating feature in junctions with metallic contacts, since, as noted above, sub-bandgap light cannot excite electron-hole pairs in a semiconductor substrate [4]. Hence, the main source of relaxation in SC-molecule-SC junctions under the conditions considered is the charge transfer between the bridge and the contacts. The interaction of a nonresonant EM field with such systems leads to modulation of their energetic spectrum by the field frequency ω [18, 19, 21]. The efficiency of the energy spectrum modulation depends on the interaction parameter $z = \mathbf{D} \cdot \mathbf{E}_0/(\hbar\omega)$, where $\mathbf{E}_0$ is the amplitude of the electromagnetic field $\mathbf{E}(t)$. The permanent dipole moment of relevant molecules can reach 10 D and more. The spectral modulation alters the arrangement of molecular electronic states and may substantially change the electron and hole transfer rates between the molecular bridge and the SC contact, due to the strong dependence of these rates on the position of the molecular level relative to the conduction band (CB) and valence band (VB). Suppose that initially a single molecular level of energy ε_i is positioned between the conduction and valence bands of

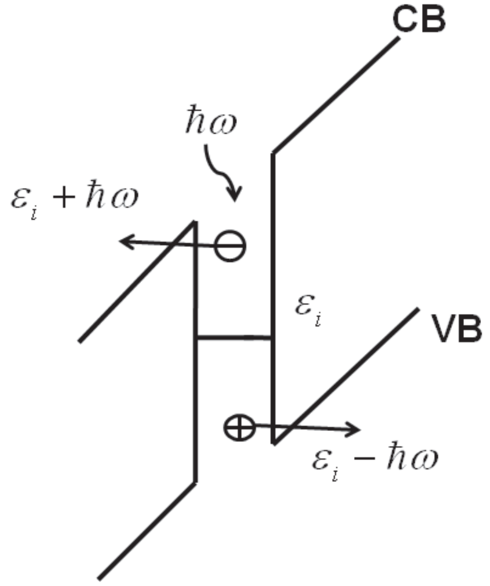

FIGURE 1. Electromagnetic excitation applied to a molecular bridge in state ε_i leads to generation of its photonic replica at energies $\varepsilon_i \pm \hbar\omega$. Tunnelling from the photonic replica results in a unidirectional photocurrent. CB - conduction band, VB - valence band.

the SC contacts shown in Fig.1. No current in such SC-molecule-SC junction is possible even in the presence of the voltage bias. If, however, an electromagnetic pulse of appropriate frequency ω excites the molecular bridge, photonic "replication" of state i with energy $\varepsilon_i + \hbar\omega$ can be tuned to be close to the CB, while the photonic "replication" with energy $\varepsilon_i - \hbar\omega$ is energetically close to the VB. In that situation a current flows through the junction and its temporal duration is controlled by the electromagnetic pulse characteristics. The transport rate is largely controlled by the applied voltage bias, which determines the barrier width (the asymmetric case, where the molecular level is remote from the gap center, is addressed in Ref.[16]). This control enables us to realize coherent excitation of a molecular bridge while circumventing competing processes.

Theory

The complete Hamiltonian describing a molecular bridge interacting with two semiconductor electrodes and subject to a low frequency optical pulse is written as, $\hat{H} = \hat{H}_{wire} + \hat{H}_{SC} + \hat{W} + \hat{V}$, where the zero order wire Hamiltonian,

$$\hat{H}_{wire} = \sum_{n=1}^{N} \varepsilon_n \hat{c}_n^\dagger \hat{c}_n - \Delta \sum_{n=1}^{N-1} (\hat{c}_{n+1}^\dagger \hat{c}_n + \hat{c}_n^\dagger \hat{c}_{n+1}) \tag{2}$$

is described as a tight-binding model composed of N sites, where each site represents available orbitals (e.g. the HOMO and/or the LUMO), ε_n denotes the electron energy on site n and $\hat{c}_n^\dagger$ ($\hat{c}_n$) are creation (annihilation) operators for electrons in site n. The Δ term in Eq. (2) accounts for electron transfer interactions between nearest sites within the Huckel model. The Hamiltonian of the intrinsic semiconductor leads is given as, $\hat{H}_{SC} = \sum_{n=1,N} \sum_{k \in K_n} (\varepsilon_{ck} \hat{c}_{ck}^\dagger \hat{c}_{ck} + \varepsilon_{vk} \hat{c}_{vk}^\dagger \hat{c}_{vk})$ where c (v) denote the conduction (valence) bands and $\varepsilon_{c(v)k}$ are the corresponding quasicontinuum electron energies. In what follows we will omit the band indices c and v when not essential, so as to simplify the notation. We denote by K_1 the lead in contact with bridge site $n = 1$ and by K_N the lead in contact with site $n = N$. $\hat{W}(t) = -\mathbf{D} \cdot \mathbf{E}(t)$ describes the interaction of the bridge sites with an external electromagnetic field $\mathbf{E}(t)$, where the dipole operator has only diagonal elements, $D_{mm} = D[\delta_{N1} + (N+1-2m)/2]$. Here D is given by the product of electron charge by the distance between the neighboring sites [1], and δ_{N1} is the Kronecker delta. Finally, $\hat{V} = \sum_{n=1,N;k \in K_n} (V_{nck} \hat{c}_{ck}^\dagger \hat{c}_n + V_{nvk} \hat{c}_{vk}^\dagger \hat{c}_n) + h.c.$, where $h.c.$ denotes Hermitian conjugate, describes electron transfer between the molecular bridge and the leads, thus giving rise to net current via the biased junction.

We consider electronic transport through the molecular wire, where the semiconductor leads K_n, $n = 1, N$ are taken to be each in its own equilibrium characterized by its temperature T (here taken equal for the two leads) and electronic electrochemical potentials $\mu_{K_n c}$ and $\mu_{K_n v}$ for the conduction and valence bands, respectively. Therefore, the lead electrons are described by the equilibrium Fermi functions $f_{K_n}(\varepsilon_{c(v)k}) = [\exp((\varepsilon_{c(v)k} - \mu_{K_n c(v)})/k_B T) + 1]^{-1}$ where k_B is Boltzmann's constant. Consequently, expectation values for lead operators are simplified through the relation $\langle \hat{c}_{c(v)k}^\dagger \hat{c}_{c(v)k'} \rangle = f_{K_n}(\varepsilon_{c(v)k}) \delta_{kk'}$.

Our analysis is based on the generalized master equation for the reduced density matrix of the molecular subsystem treating $\hat{V}$ as a perturbation [1, 22, 23]. Briefly, one starts with the equation of motion for the total density operator and uses projectors onto the left (L) and right (R) quasicontinua of the type $P_K \rho(t) = \rho_K \mathrm{Tr}_K \rho(t)$, $K = L, R$, in order to derive an equation for the time evolution of the reduced density matrix $\sigma(t) = \mathrm{Tr}_R \mathrm{Tr}_L \rho(t)$ [17, 16].

Single site molecular bridge

In this section we specialize the theory developed in the previous section to the simplest case scenario of a single site bridge. We illustrate a new and fundamentally interesting phenomenon, namely zeros of the light-induced currents as a function of the interaction strength, which are reminiscent of the phenomenon of coherent destruction of tunneling [24, 1, 5], and which we term coherent destruction of induced tunneling (CDIT).

Using the equation of motion for σ [17, 16], one obtains relations for the expectation values of the molecular bridge operators $P_{i'i} = \langle \hat{c}_i^\dagger \hat{c}_{i'} \rangle \equiv \mathrm{Tr}(\hat{c}_i^\dagger \hat{c}_{i'} \sigma) = P^*_{ii'}$ that are binary in the creation and annihilation operators for electrons in the molecular states. The time evolution of the molecular bridge population P_{ii} reduces under the conditions of Fig.1 to,

$$\frac{dP_{ii}}{dt} = \sum_n [2(1-P_{ii})\Gamma_{vK_n,i} - 2P_{ii}\Gamma_{cK_n,i}] \tag{3}$$

where

$$\Gamma_{vK_n,i} = \sum_{r=1}^{\infty} J_r^2(z_i)\gamma^{rr}_{vK_n,i}, \Gamma_{cK_n,i} = \sum_{r=-\infty}^{-1} J_r^2(z_i)\gamma^{rr}_{cK_n,i}, \tag{4}$$

$\omega_i = \varepsilon_i/\hbar$, $z_i = \mathbf{D}_{ii} \cdot \mathbf{E}_0/(\hbar\omega)$, and

$$\gamma^{rr}_{c,vK_n,i} = \frac{\pi}{\hbar^2}\sum_k |V_{c,vki}|^2 \delta(\omega_k - \omega_i + r\omega) \tag{5}$$

are the spectral functions, which take the significance of replication-specific decay rates due to coupling of the bridge site with the conduction (c) and the valence (v) band of the electrode. For the specific model depicted in Fig.1, $\gamma^{11}_{vL,i} = \gamma^{-1,-1}_{cR,i} = 0$, and, given that only a single site is included ($N = 1$), we replaced the K_n, $n = 1,N$ notation by $K_1 = L$ for the left electrode and $K_N = R$ for the right electrode of the single site junction.

Equation (4) describes the rate of electron transfer between the molecular state i and the conduction (valence) bands ($\Gamma_{c(v)L(R),i}$) as a sum over contributions of electron transfer rates $\gamma^{rr}_{c(v)R(L),i}$, in which the underlying potential coupling constants $V_{c(v)ki}$ are evaluated in the absence of the laser field but the energy-conserving δ-function tunes the electron energy to the r-photonic replication, that is, to the side-band energy $\hbar\omega_i \pm |r|\hbar\omega$ shifted by integer multiples of the photon quantum. The dependence on the interaction strength, $z_i = \mathbf{D}_{ii} \cdot \mathbf{E}_0/(\hbar\omega)$, is solely contained in the squared Bessel functions in Eq. (4), which serve as weight functions for the $\gamma^{rr}_{c(v)R(L),i}$ components of $\Gamma_{c(v)L(R),i}$. Note that the partial electron transfer rates $J_r^2(z_i)\gamma^{rr}_{cL(R),i}$ and $J_r^2(z_i)\gamma^{rr}_{vL(R),i}$ contain contributions from negative and positive r-values, respectively. Thus, the photon absorption ($r < 0$) and emission ($r > 0$) processes can be viewed as creating effective molecular states at energies $\hbar\omega_i + r\hbar\omega$ with probabilities $J_r^2(z_i)$. These probabilities decay rapidly with r when $|z_i| < 1$.

The electronic current $I_{L,R}$ is given by [17, 16]

$$I_K = -2e[(1-P_{ii})\Gamma_{vK,i} - P_{ii}\Gamma_{cK,i}]. \tag{6}$$

The first order differential equation (3) can be readily integrated. In the steady-state limit we get

$$I_L = -I_R = 2eJ_1^2(z_i)\frac{\gamma^{-1,-1}_{cL,i}(\Gamma_{vR,i} - \gamma^{11}_{vR,i}) + \gamma^{11}_{vR,i}\Gamma_{cL,i}}{\Gamma_{vi} + \Gamma_{ci}}. \tag{7}$$

i.e., as expected, under steady state conditions the currents are equal. Here $\Gamma_{vi} = \sum_{K_n}\Gamma_{vK_n,i}$ and $\Gamma_{ci} = \sum_{K_n}\Gamma_{cK_n,i}$ are the rates of electron transfer between the molecular state i and the valence and conduction bands, respectively, of the two leads, and we used Eq.(6). For broad conduction and valence bands and $|r| > 1$, it may be expected that, due to symmetry, the spectral functions of the r-th order replication would be equal for the left and right contacts, i.e. $\gamma^{rr}_{cL,i} = \gamma^{rr}_{cR,i}$ and $\gamma^{rr}_{vR,i} = \gamma^{rr}_{vL,i}$ that we took into account when derived Eq. (7).

Equation (7) shows that a steady-state current is proportional to the square of the first-order Bessel function $J_1^2(z_i)$. This implies that the current vanishes identically at zeros of $J_1(z_i)$ (i.e. for $z_i = 0,\ 3.8,\ 7, \ldots$). The phenomenon observed in Eq. (7) is referred to in what follows as coherent destruction of induced tunneling (CDIT), as it extends the extensively studied problem of coherent destruction of tunneling (CDT), related to zeros of $J_0(z_i)$ [24, 1, 5] to the case of light-induced tunneling. In the present case the effect could be formulated as dressing of the laser-free coupling of the molecular bridge with semiconductor leads, $V_{c(v)ki}$, by the light field to make the effective coupling,

$$V_{c(v)ki} \rightarrow (V_{c(v)ki})_{eff} = J_{\mp 1}(z_i)V_{c(v)ki}$$

for the electron transfer rates $\gamma^{-1,-1}_{cL,i}$ and $\gamma^{11}_{vR,i}$ (see Eq.(7)). These effective tunneling matrix elements $(V_{c(v)ki})_{eff}$ are suppressed at zeros of $J_{\mp 1}(z_i)$.

A two-site molecular bridge

In this section we consider the case of a two-site molecular bridge in contact with SC leads. Specifically, we envision two molecular sites of energies ε_1 and ε_2 (Fig.2) that are excited by EM field $\mathbf{E}(t) = \mathbf{E}_0\cos(\omega t)$ tuned to a sub-bandgap frequency ω, such that the dressed energies $\varepsilon_{1,2} + \hbar\omega$ and $\varepsilon_{1,2} - \hbar\omega$ are close to the conduction and valence bands, respectively. The sites are coupled to each other due to the intersite interaction Δ of Eq.(2), and interact with the EM field due

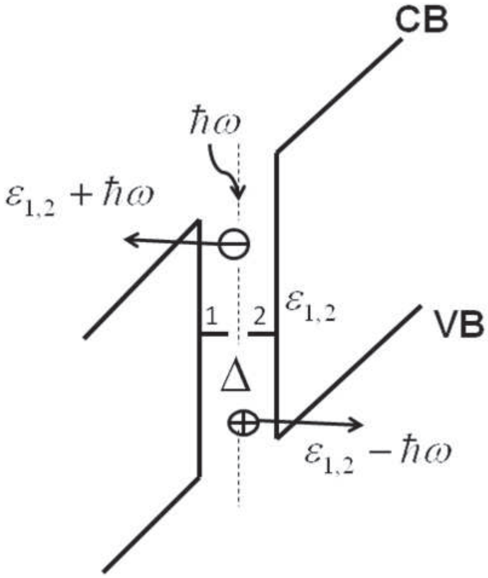

FIGURE 2. Two-site molecular bridge. The sites are coupled to each other due to intersite interaction Δ, and posses permanent dipole moments $\mathbf{D}_{11}=-\mathbf{D}_{22}\equiv\mathbf{D}/2$.

to site permanent dipole moments $\mathbf{D}_{11}=-\mathbf{D}_{22}\equiv\mathbf{D}/2$ [1, 5] (see Sec.Model). In the limit of a small energy gap $|E_2-E_1|/\hbar$ and weak coupling $\Delta/\hbar$,

$$\hbar\omega \gg |\Delta|, |E_2-E_1|, \tag{8}$$

one can obtain the equations for the expectation values of the molecular bridge operators, the polarization P_{12} and the populations P_{nn}, $n=1,2$ that, in turn, determine the light-induced hole and the electron currents in the two-site junction [16]. In particular,

$$\begin{aligned}\frac{dP_{12}}{dt}+i(\bar{\omega}_{12}-\frac{\mathbf{D}\cdot\mathbf{E}}{\hbar})P_{12}+\frac{i}{\hbar}\Delta(P_{11}-P_{22})\\ =-P_{12}(\Gamma_{vL,1}+\Gamma_{cL,1}+\Gamma_{vL,2}+\Gamma_{cL,2})\end{aligned} \tag{9}$$

and

$$\begin{aligned}\frac{dP_{nn}}{dt}+\frac{2}{\hbar}(-1)^n\Delta ImP_{12}\\ =2\Gamma_{vK_n,n}(1-P_{nn})-2\Gamma_{cK_n,n}P_{nn}\end{aligned} \tag{10}$$

Similar to Ref.[23], we define the electronic current I for two-sites case as the rate of change of electron population on the left of the dashed line in Fig. 2,

$$I=\frac{ie}{\hbar}\Delta(P_{21}-P_{12})=\frac{2e}{\hbar}\Delta ImP_{12}. \tag{11}$$

The set of first order differential equations (10) and (9) can be integrated for excitation by a rectangular pulse [16]. In the long time limit the current approaches its steady-state value,

$$I_{SS}=\frac{e\Delta^2J_0^2(z)J_1^2(z_2)\gamma_{vR,2}^{11}}{\Delta^2J_0^2(z)+(\hbar^2/4)(\Gamma_{L1}+\Gamma_{R2})^2}, \tag{12}$$

where $z=\mathbf{D}\cdot\mathbf{E}_0/(\hbar\omega)$; $\Gamma_{L1}=\Gamma_{vL,1}+\Gamma_{cL,1}$ and $\Gamma_{R2}=\Gamma_{vR,2}+\Gamma_{cR,2}$ denote the rates of electron transfer between molecular state $j=1,2$ and the corresponding lead, and we used Eq.(11) and put $\bar{\omega}_{12}=0$ for simplicity. In deriving Eq. (12), we assumed that the spectral functions of r-th order for a given band are equal for the left and right contacts, i.e.

$$\gamma_{cL,i}^{rr}=\gamma_{cR,j}^{rr}, \gamma_{vR,i}^{rr}=\gamma_{vL,j}^{rr} \tag{13}$$

for $i\neq j$ when $|r|>1$, and that (as above)

$$\gamma_{vR,2}^{11}=\gamma_{cL,1}^{-1,-1}. \tag{14}$$

In particular, as discussed before, the former assumption is expected to hold due to symmetry in the case of broad conduction and valance bands. When the relations given by Eqs.(13) and (14) are realized, the rates of electron transfer Γ_{L1} and Γ_{R2} are equal, $\Gamma_{L1}=\Gamma_{R2}$.

The steady-state current for a two-site molecular bridge, Eq.(12), is proportional to the square of the product of zero- and first-order Bessel functions $J_0(z)J_1(z_2)$ of different arguments z and $z_2=-z/2$. Consequently, the current vanishes at zeros of both $J_0(z)$ and $J_1(-z/2)$ (i.e. for the values of $|z|=0$, 2.4, 5.52, 7.6, 8.65,...). Thus, the phenomenon of CDIT for a two-site molecular bridge differs qualitatively from both CDIT for a single site bridge and the conventional CDT. In particular, for the 2-site bridge, both the coupling of the molecular bridge with semiconductor leads $V_{c(v)kj}$ and the electron hopping matrix element Δ are replaced through the interaction with the light by their effective values, $V_{c(v)kj}\rightarrow(V_{c(v)kj})_{eff}=J_{\mp1}(z_j)V_{c(v)kj}$ and $\Delta\rightarrow\Delta_{eff}=J_0(z)\Delta$ (see Eq.(12)). The corresponding effective tunneling matrix elements $(V_{c,vkj})_{eff}$ and Δ_{eff} vanish at zeros of $J_{\mp1}(z_j)$ and $J_0(z)$, respectively.

To determine the steady-state current versus z, Eq.(12), one needs to know z-dependence of $\Gamma_{L1}+\Gamma_{R2}$, which requires calculation of the rates $\gamma_{c,vKj}^{rr}$, Eq.(5), as functions of r, the order of the photonic replication. Using the density of states of a 3D semiconductor, one obtains for $|r|\geq2$

$$\gamma_{c,vK_j,j}^{rr}=\sqrt{|r|-1}\,\gamma_{c,vK_j,j}^{\mp2,\mp2}, \tag{15}$$

with which $\Gamma_{R2}=\Gamma_{L1}$ and

$$\Gamma_{R2}=J_1^2(\frac{z}{2})\gamma_{vR,2}^{11}+(\gamma_{vR,2}^{22}+\gamma_{cR,2}^{-2,-2})\sum_{r=2}^{\infty}J_r^2(\frac{z}{2})\sqrt{r-1} \tag{16}$$

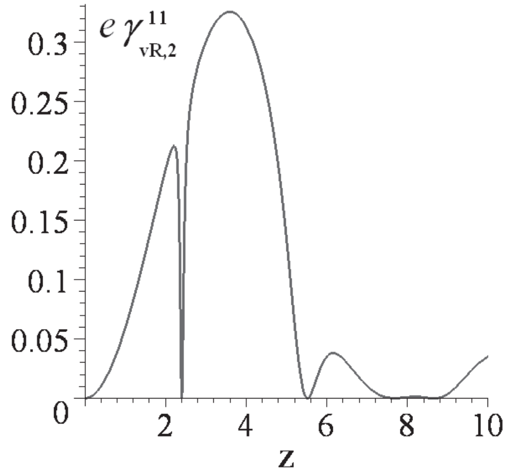

FIGURE 3. Steady-state current for two-site bridge versus z, calculated using Eqs.(12) and (16) for $\gamma^{22}_{vR,2}+\gamma^{-2,-2}_{cR,2}=10\gamma^{11}_{vR,2}$ and $\hbar\gamma^{11}_{vR,2}/|\Delta|=0.054$.

where we used Eqs.(4), (13) and (14). A plot of I_{SS} versus z is provided in Fig.3, illustrating that the steady-state current for the two-site bridge vanishes at both the zeros of the current corresponding to CDT and the zeros of the induced current for a single site bridge. We note also the qualitative difference between the currents for the single- and the double-site bridges, originating from the differences of the underlying electronic dynamics.

PHOTON ASSISTED CURRENT IN MOLECULAR NANOJUNCTIONS WITH GRAPHENE CONTACTS [25]

In the second part of our work, as a first step, we calculate a semiclassical wave function of a doped graphene under the action of EM excitation. Then we obtain Heisenberg equations for the second quantization operators of graphene and calculate current through a molecular junction with graphene electrodes using non-equilibrium Green functions (GF). We address different cases, which are analytically soluble, hence providing useful insights.

Calculation of Semiclassical Wave Function

The states of electrons in graphene are conveniently described by the four-component wave functions, defined on two sublattices and two valleys. Electron motion in the time-dependent EM field is described by the 2D Dirac equation [12, 13]

$$i\hbar\frac{\partial\psi}{\partial t}=[v\hat{\sigma}(\hat{\mathbf{p}}-\frac{e}{c}\mathbf{A})+e\varphi_{pot}]\psi \qquad (17)$$

written for a single valley and for a certain direction of spin. Here $\hat{\mathbf{p}}$ is the momentum of the quasiparticle, v - the Fermi velocity ($v\approx 10^6$ m/s), $\hat{\sigma}$ - the vector of the Pauli matrices in the sublattice space ("pseudospin" space), $\mathbf{A}$ and φ_{pot} are vector and scalar potentials of an EM field, respectively. Suppose a graphene film is excited by a linearly polarized monochromatic electric field $E_x(t)=E_0\cos\omega t$ that is parallel to its plane (x,y). Then $A_x=-(c/\omega)E_0\sin\omega t$, $A_y=A_z=0$. To obtain a semiclassical solution of Eq.(17), we use a method of Ref. [26] (see also [27]). As a result, we get the wave function normalized for the graphene sheet area s [25]:

$$\psi=\frac{1}{\sqrt{s}}\exp(ip_xx/\hbar+ip_yy/\hbar)\exp[\frac{i}{\hbar}(\mp v\int_0^t\bar{p}dt'-$$
$$-e\int_0^t\varphi_{pot}dt')]\bar{u}_{\mathbf{p}\pm} \qquad (18)$$

where $\bar{\mathbf{p}}$ is the normal momentum that obeys the classical equations of motion for a particle with charge $-e$, according to which $\bar{p}_x(t)=-(eE_0/\omega)\sin(\omega t)$; $\bar{\mathbf{p}}=\mathbf{p}-\frac{e}{c}\mathbf{A}$ where $\mathbf{p}$ is the generalized momentum. Here slowly varying spinors $\bar{u}_{\mathbf{p}\pm}$ are equal to

$$\bar{u}_{\mathbf{p}\pm}=\frac{1}{\sqrt{2}}\begin{pmatrix}\exp(-i\bar{\varphi}/2)\\ \pm\exp(i\bar{\varphi}/2)\end{pmatrix}, \qquad (19)$$

$\bar{p}\equiv|\bar{\mathbf{p}}(t)|$, $\tan\bar{\varphi}=\bar{p}_y/\bar{p}_x$, $p_x=p\cos\varphi$, $p_y=p\sin\varphi$, $\tan\varphi=p_y/p_x$. In the absence of external EM field Eqs.(18) and (19) give the exact wave function of unperturbated graphene [12]. Eqs.(18) and (19) show remarkable and very simple result, according to which the time-dependent part of the semiclassical wave function is defined by the same formula as that for the unperturbated system with the only difference that the generalized momentum $\mathbf{p}$ should be replaced by the usual momentum $\bar{\mathbf{p}}$. The space-dependent part of the wave function remains unchanged.

The wave function of the graphene sheet interacting with molecular bridge Ψ may be represented as the superposition of wave functions, Eqs.(18) and (19). Passing to the second quantization, we get

$$\Psi = \frac{1}{\sqrt{s}}\sum_{+,-}\sum_{\mathbf{p}}\hat{a}_{\mathbf{p}\pm}\exp[\tfrac{i}{\hbar}\mathbf{pr}+\tfrac{i}{\hbar}(\mp v\textstyle\int_0^t\bar{p}dt'$$
$$-e\textstyle\int_0^t\varphi_{pot}dt')]\bar{u}_{\mathbf{p}\pm} \qquad (20)$$

where $\hat{a}_{\mathbf{p}\pm}$ are annihilation operators. To obtain the Hamiltonian in the second quantization representation, consider an average energy of a particle with wave function ψ that is given by $\int\psi^*\hat{H}\psi d\mathbf{r}=i\hbar\int\psi^*(\partial\psi/\partial t)d\mathbf{r}$.

Replacing wave functions ψ for Ψ operators and integrate with respect to $\mathbf{r}$, we get

$$\hat{H} = \int \Psi^{\dagger}\hat{H}\Psi d\mathbf{r} = \sum_{\mathbf{p}\sigma}\sum_{+,-}\hat{a}^{\dagger}_{\mathbf{p}\pm,\sigma}\hat{a}_{\mathbf{p}\pm,\sigma}[\pm v\bar{p}(t) + e\varphi_{pot}(t)] \tag{21}$$

where $\sum_{\sigma}\hat{a}^{\dagger}_{\mathbf{p}\pm,\sigma}\hat{a}_{\mathbf{p}\pm,\sigma} = \hat{a}^{\dagger}_{\mathbf{p}\pm}\hat{a}_{\mathbf{p}\pm}$, $\sigma = 1,2$ is the "quasispin" index. Using Hamiltonian, Eq.(21), we obtain the Heisenberg equations of motion

$$\frac{d\hat{a}_{\mathbf{p}\pm,\sigma}(t)}{dt} = \frac{i}{\hbar}[\hat{H}, \hat{a}_{\mathbf{p}\pm,\sigma}] \simeq \frac{i}{\hbar}[\mp v\bar{p}(t) - e\varphi_{pot}(t)]\hat{a}_{\mathbf{p}\pm,\sigma}(t) \tag{22}$$

Formula for the Current

Consider a spinless model for a molecular wire that comprises one site of energy ε_m, positioned between either both graphene electrodes (leads) or one graphene and another one - a metal electrode. The corresponding Hamiltonian is $\hat{H}_{wire} + \hat{H}_{leads} + \hat{V}$ where the wire Hamiltonian is $\hat{H}_{wire} = \varepsilon_m \hat{c}^{\dagger}_m \hat{c}_m$, $\hat{c}^{\dagger}_m$ ($\hat{c}_m$) are creation (annihilation) operators for electrons at the molecular wire. The molecule-leads interaction $\hat{V}$ describes electron transfer between the molecular bridge and the right (R) and left (L) leads that gives rise to net current in the biased junction

$$\hat{V} = \sum_{+,-}\sum_{\sigma,\mathbf{p}\in\{L,R\}}(V_{\mathbf{p}\pm,\sigma;m}\hat{a}^{\dagger}_{\mathbf{p}\pm,\sigma}\hat{c}_m + H.c.), \tag{23}$$

Here $H.c.$ denotes Hermitian conjugate. The current from the K lead ($K = L, R$) can be obtained by the generalization of Eq.(12.11) of Ref.[28]

$$I_K = -\frac{2\kappa e}{\hbar}\sum_{+,-}\sum_{\sigma,\mathbf{p}\in K} V_{\mathbf{p}\pm,\sigma;m} Re[G^{<}_{m;\mathbf{p}\pm,\sigma}(t,t)] \tag{24}$$

where $\kappa = 1$ for the metal electrode, and $\kappa = 2$ for the graphene electrode that accounts for the valley degeneracies of the quasiparticle spectrum in graphene. $G^{<}_{m;\mathbf{p}\pm,\sigma}(t,t') = i\langle \hat{a}^{\dagger}_{\mathbf{p}\pm,\sigma}(t')\hat{c}_m(t)\rangle$ denotes the lesser GF. Calculating the latter, we get [25]

$$I_K = \frac{4e}{\hbar}\int_{-\infty}^{t} dt_1 \sum_{+,-} Im \int_0^{\infty}\frac{d(vp)}{2\pi}\exp[\pm\frac{i}{\hbar}e\varphi_{pot,K}(t-t_1)]$$
$$\times \Gamma^K_{mm}(\pm vp, t_1, t)[G^r_{mm}(t,t_1) f^K(\pm vp) + G^{<}_{mm}(t,t_1)] \tag{25}$$

where $G^r_{mm}(t,t_1)$ and $G^{<}_{mm}(t,t_1)$ are the retarded and lesser wire GFs, respectively; $f^K(vp_{\pm}) \equiv \langle \hat{a}^{\dagger}_{\mathbf{p}\pm,\sigma}(0)\hat{a}_{\mathbf{p}\pm,\sigma}(0)\rangle = \left[1 + \exp\left(\frac{\pm vp - \mu_K}{k_B T}\right)\right]^{-1}$ is the Fermi function and μ_K - the chemical potential of lead K, and

$$\Gamma^K_{mm}(\pm vp, t_1, t) = \frac{s}{\pi\hbar^2 v^2}\sum_{\sigma\in K}\int_0^{\pi} d\theta\, vp V_{\mathbf{p}\pm,\sigma;m}(t)$$
$$\times V^{*}_{\mathbf{p}\pm,\sigma;m}(t_1)\exp[\pm\frac{i}{\hbar}v\int_{t_1}^{t} dt'\bar{p}(t')] \tag{26}$$

is the level-width function. To proceed, we shall make the time expansion of $\Gamma^K_{mm}(\pm vp, t_1, t)$ into the Fourier series, and then use the Markovian approximation, considering time $t - t_1 \equiv \tau$ as very short. This will also enable us to use the non-interacting resonant-level model [28] for finding the time dependence of $G^r_{mm}(t, t-\tau)$ and $G^{<}_{mm}(t, t-\tau) = in_m(t)\exp(-\frac{i}{\hbar}\varepsilon_m\tau)$ as functions of t and $t-\tau$ where $n_m(t)$ is the population of molecular state m. According to the Floquet theorem [1], the general solution of the Schrödinger equation for an electron subjected to a periodic perturbation, takes the form $\psi(t) = \exp(-\frac{i}{\hbar}\varepsilon t)\Phi_T(t)$, where $\Phi_T(t)$ is a periodic function having the same period T as the perturbation, and ε is called quasienergy. Then the expansion of function $\exp[\frac{i}{\hbar}v\int_0^t dt'\bar{p}(t')]$ on the right-hand side of Eq.(18) into the Fourier series will be as following

$$\exp[\frac{i}{\hbar}v\int_0^t dt'\bar{p}(t')] = \exp[\frac{i}{\hbar}\varepsilon(p,\theta)t]\sum_{l=-\infty}^{\infty} c_l(p,\theta)\exp(ilt\omega) \tag{27}$$

where

$$c_l(p,\theta) = \frac{\omega}{2\pi}\int_{-\frac{\pi}{\omega}}^{\frac{\pi}{\omega}}\exp[\frac{iv}{\hbar}\int_0^t \bar{p}dt' - \frac{i}{\hbar}\varepsilon(p,\theta)t - il\omega t]dt \tag{28}$$

Using expansion, Eq.(27), into Eq.(26) and neglecting fast oscillating with time t terms, we get

$$\Gamma^K_{mm}(\pm vp, \tau) = \frac{s}{\pi\hbar^2 v^2}\sum_{\sigma\in K}\int_0^{\pi} d\theta\, vp|V_{\mathbf{p}\pm,\sigma;m}|^2$$
$$\times \sum_{n=-\infty}^{\infty}|c_n(p,\theta)|^2\exp\{\pm i[\frac{\varepsilon(p,\theta)}{\hbar} + n\omega]\tau\} \tag{29}$$

Then going to the integration with respect to τ in Eq.(25) and bearing in mind Eq.(29), we get

$$I_K = 4e\sum_{\sigma\in K}\int_0^{\pi} d\theta \sum_{n=-\infty}^{\infty}[n_m(t) - f^K(vp_{n\pm})]$$
$$\times |c_n(p_{n\pm},\theta)|^2\bar{\gamma}^{(n)\pm}_{G_K\sigma,m} \tag{30}$$

where we denoted

$$\bar{\gamma}^{(n)\pm}_{G_K\sigma,m} = \frac{s}{2\pi\hbar^3 v^2}\int_0^{\infty} vpd(vp)|V_{\mathbf{p}\pm,\sigma;m}|^2 \times$$
$$\times \delta[\pm(\varepsilon(p,\theta) + n\hbar\omega) + e\varphi_{pot,K} - \varepsilon_m] \tag{31}$$

is the spectral function for the n-th photonic replication, $\delta(x)$ is the Dirac delta, arguments $p_{n\pm}$ are defined by equation

$$\varepsilon_{\pm}(p,\theta) = \pm(\varepsilon_m - e\varphi_{pot,K}) - n\hbar\omega \tag{32}$$

and should be positive. Below we shall consider $V_{\mathbf{p}\pm,\sigma;m}$ not dependent on $\mathbf{p}\pm$ and quasispin σ.

Molecular bridge between graphene and metal electrodes

Consider a specific case when the molecular bridge is found between graphene and metal (tip) electrodes. In that case one can use Eq.(30) for $K = L$:

$$I_L = 4e \sum_{\sigma\in K} \sum_{n=-\infty}^{\infty} [n_m(t) - f^L(vp_{n\pm})] \times \int_0^{\pi} d\theta |c_n(p_{n\pm},\theta)|^2 \bar{\gamma}^{(n)\pm}_{G_L\sigma,m} \tag{33}$$

If R represents the metal electrode, then

$$I_R = 2e\gamma_{Rm}[n_m(t) - f^R_{\mathbf{p}}] \tag{34}$$

where $2\gamma_{Rm}$ is the charge transfer rate between the molecular bridge and the metallic lead. In the case under consideration the equation for $n_m(t)$ becomes

$$dn_m/dt = -I_L/e - I_R/e \tag{35}$$

that is written as the continuity equation. Inserting Eqs.(33) and (34) into Eq.(35), solving the latter for the steady-state regime and substituting the solution into Eq. (34), we get

$$I_R = 4e\sum_{n\sigma} \int_0^{\pi} d\theta |c_n(p_{n\pm},\theta)|^2 \bar{\gamma}^{(n)\pm}_{G_L\sigma,m} [f^L(vp_{n\pm}) - f^R_{\mathbf{p}}] \tag{36}$$

for a special case

$$\gamma_{Rm}/2 >> \textstyle\sum_\sigma \sum_{n=-\infty}^{\infty} \bar{\gamma}^{(n)\pm}_{G_L\sigma,m} \int_0^{\pi} d\theta |c_n(p_{n\pm},\theta)|^2$$

Eq.(36) seems similar to that of Tien and Gordon, Eq.(1), and generalizes it. To calculate current, we shall use a variety of approaches.

Function $\exp[\frac{i}{\hbar} v \int_0^t dt' \bar{p}(t')]$ may be written in the dimensionless form as $\exp(i\frac{\alpha}{b} \int_0^y dx \sqrt{1 + 2b\cos\theta \sin x + b^2 \sin^2 x})$ where $b \equiv (eE_0 v/\omega)/(vp)$ and $\alpha = (eE_0 v/\omega)/(\hbar\omega)$ represent the work done by the electric field during one fourth of period weighted per unperturbated energy vp and photon energy $\hbar\omega$, respectively; $y = \omega t$, and we assume $eE_0 > 0$. If $b < 1$, one can use the cumulant expansion, and we get $\exp[i\frac{\alpha}{b} \int_0^y dx \sqrt{1 + 2b\cos\theta \sin x + b^2 \sin^2 x}] = \exp[G_1(y) + G_2(y)]$, where $G_1(y)$ contains only a constant term and the linear with respect to y term that describes the quasienergy weighted per photon energy [25]. The term $\exp[G_2(y)]$ can be expanded in terms of the Bessel functions $J_s(z_i)$ [29]. In case of large momenta (far from the Dirac point), $b << 1$, $\varepsilon(p,\theta) \approx vp$, and we get from Eq.(32): $vp_{n\pm} = \pm(\varepsilon_m - e\varphi_{pot,K}) - n\hbar\omega$. In that case quantities $\bar{\gamma}^{(n)\pm}_{G_L\sigma,m}$, Eq.(31), become

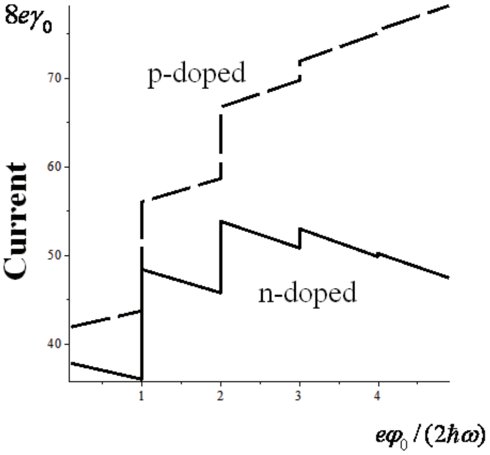

FIGURE 4. Current in the case of large momenta for n-doped ($\mu > 0$, solid) and p-doped ($\mu < 0$, dashed) graphene electrode as a function of applied voltage bias. $|\varepsilon_m| = 20\hbar\omega$, $\alpha = 3$.

$$\bar{\gamma}^{(n)\pm}_{G_L\sigma,m} = \frac{\gamma_0}{\pi}[\pm\frac{(\varepsilon_m - e\varphi_{pot,L})}{\hbar\omega} - n] \tag{37}$$

where $\gamma_0 = |V_{\mathbf{p}\pm,\sigma;m}|^2 s\omega/(2\hbar^2 v^2)$, and the expression in the square brackets is proportional to the DOS for graphene that is proportional to energy [12]. In the case under consideration, $|c_l(p,\theta)|^2 = J_l^2(\alpha\cos\theta)$ [25]. The current, Eq.(36), calculated for large momenta when $\alpha = 3$, as a function of applied voltage bias is shown in Fig.4. In our calculations temperature $T = 0$, and the leads chemical potentials in the biased junction were taken to align symmetrically with respect to the energy level ε_m [30], i.e., $\mu + e\varphi_0/2$ for the left lead, and $\mu - e\varphi_0/2$ for the right lead ($e\varphi_0 \geq 0$, $e\varphi_{pot,(L,R)} = \pm e\varphi_0/2$) where $\mu = \varepsilon_m$ for both leads. Both curves of Fig.4 show photon assisted current - the steps when the potential of the graphene electrode achieves the values corresponding to integer multiples of the photon energy. The steps are found on the background that decreases linearly for a n-doped graphene electrode and increases linearly for a p-doped electrode when $e\varphi_0$ increases. This is related to the linear dependence of DOS on energy. To calculate coefficients $c_l(p,\theta)$, Eq.(28), in general case, we need to know quasienergy $\varepsilon(p,\theta)$. The latter may be found as zero harmonic of the Fourier cosine series of normal momentum $\bar{p}(t)$ on the left-hand side of Eq.(28). Consider first limiting points $\theta = 0,\pi$ when the momentum is parallel to the electric field. Then the quasienergy

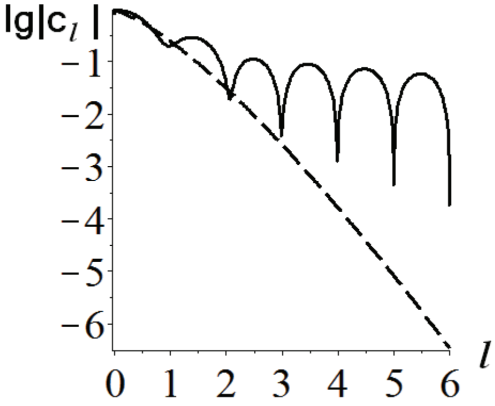

FIGURE 5. The logarithm of the absolute values of Fourier-coefficients $c_l(p;\theta=0,\pi)$ (solid line) versus harmonic number l for n-doped graphene contact ($\mu>0$) and $\alpha=0.5$, $b=1.43>1$. For comparison we also show $|J_l(\alpha)|$ (dashed line). We use the continuous variable l though l takes only the whole values.

weighted per the work done by the electric field during one fourth of period is equal to $\bar{\varepsilon}(p;\theta=0,\pi)\equiv\varepsilon(p;\theta=0,\pi)/(evE_0/\omega)=[1/(2\pi b)]\int_{-\pi}^{\pi}dx|1\pm b\sin x|$. If $b<1$, $\bar{\varepsilon}(p;\theta=0,\pi)=1/b\sim vp$ like above. When $b>1$,

$$\bar{\varepsilon}(p;\theta=0,\pi)=\frac{2}{\pi b}[\arcsin(\frac{1}{b})+\sqrt{1-\frac{1}{b^2}}] \qquad (38)$$

that gives for $b>>1$

$$\varepsilon(p;\theta=0,\pi)=\frac{1}{\pi}[2\alpha\hbar\omega+\frac{(vp)^2}{evE_0/\omega}] \qquad (39)$$

- a quadratic dependence of $\varepsilon(p;\theta=0,\pi)$ on vp for small vp or large evE_0/ω accompanied by opening the gap $4\alpha\frac{\hbar\omega}{\pi}$ (see Fig.6 below). This gap is different from those predicted in Refs.[13, 31], which are induced by interband transitions in an undoped graphene. In contrast, a semiclassical approximation used in our work is correct for doped graphene when $\hbar\omega<2\mu$ [15], and as a consequence, interband transitions are excluded. Therefore, in our case the gap is induced by intraband processes. When $\varepsilon(p;\theta=0,\pi)$ is defined by Eq.(39), quantities $\bar{\gamma}^{(n)\pm}_{G_L\sigma,m}$, Eq.(31), become $\bar{\gamma}^{(n)\pm}_{G_L\sigma,m}=\alpha\gamma_0/4$ that do not depend on n and are proportional to α. Fig.5 shows the logarithm of the absolute values of Fourier-coefficients $c^{+}_{l}(p;\theta=0,\pi)$ for different l calculated using Eqs.(28), (32) and (38). For comparison we also show the usual dependence $|c_l(p;\theta=0,\pi)|=|J_l(\alpha)|$. One can see much slower falling down $\left|c^{+}_{l}(p;\theta=0,\pi)\right|$ with harmonics index l in comparison to the usual dependence that may be explained by the peculiarities of the graphene spectrum. One can show that $|c_l(p,\theta|$ falls down as $1/l$ for $b>>1$ and $\alpha<<1$. Such a behaviour is due to stronly non-linear EM response of graphene, which could also work as a frequency multiplier [15]. Our approach enables us to understand the origin of this non-linear response that arises due to modification of graphene gapless spectrum in the external EM field.

Consider now the middle point $\theta=\pi/2$ when the momentum is perpendicular to the electric field. In that case one can show that

$$\begin{aligned}\bar{\varepsilon}(p;\theta=\pi/2)&=\frac{1}{2\pi b}\int_{-\pi}^{\pi}dx\sqrt{1+b^2\sin^2 x}=\\&=\frac{2}{\pi}\sqrt{1+b^{-2}}E[(1+b^{-2})^{-1/2}]\end{aligned} \qquad (40)$$

where $E(x)$ is the complete elliptic integral of the second kind [29]. If $b\ll 1$, $\bar{\varepsilon}(p,\pi/2)=1/b$ like before. When $b>>1$, we get

$$\varepsilon(p,\theta=\frac{\pi}{2})=\frac{1}{\pi}\{2\alpha\hbar\omega+[\frac{1}{2}+2\ln(2\sqrt{\frac{eE_0}{\omega p}})]\frac{(vp)^2}{evE_0/\omega}\} \qquad (41)$$

where the dependence of $\varepsilon(p,\pi/2)$ on p for small p (or large eE_0/v) differs from quadratic one (cf. with Eq.(39)). Hence, the quasienergy becomes anisotropic, however, its formation is accompanied by opening the same dynamical gap $4\alpha\frac{\hbar\omega}{\pi}$ as for $\theta=0,\pi$. Quasienergies $\bar{\varepsilon}(p;\theta=0,\pi,\pi/2)$ defined by Eqs.(38) and (40) as functions of $1/b=vp/(eE_0v/\omega)$ are shown in Fig.6. They are equal to $2/\pi$ for zero momentum, then increase as $\sim(vp)^2$ for $\theta=0,\pi$, Eq.(39), and according to Eq.(41) for $\theta=\pi/2$. The law, Eq.(38), for $\theta=0,\pi$ gives way to linear one when $1/b=1$, and quasienergy for $\theta=\pi/2$ also tends to linear one when $1/b>>1$ (large momenta).

CONCLUSION

In this work, we proposed viable approaches to coherent control of electric transport via molecular junctions and developed a theoretical framework to explore the methods. Our first approach makes use of semiconducting electrodes and sub-bandgap frequencies to circumvent substrate-mediated processes and competing energy transfer events. It relies on a simple and general concept, namely the controllable photonic replication of molecular levels through interaction of the molecular permanent dipole vector with an electromagnetic field. By exploring simple, analytically soluble limits for a single and two-site molecular bridge, we showed that, acting in conjunction with the bias voltage, the electromagnetic field induces unidirectional current in the junction, whose rate is determined primarily by the bias voltage while its temporal characteristics are controlled by the laser pulse. We also predicted the phenomenon of coherent destruction

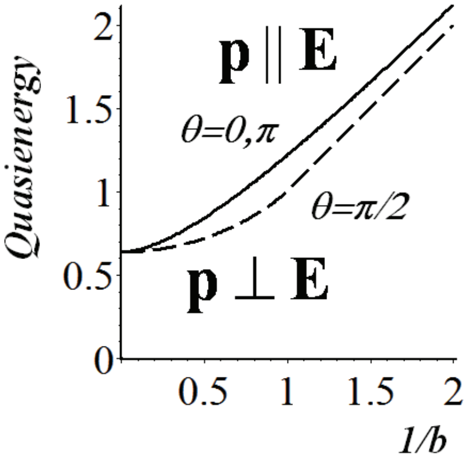

FIGURE 6. Quasienergies $\bar{\varepsilon}(p;\theta)$ for $\theta = 0,\pi$ (solid line) and $\pi/2$ (dashed line) as functions of $1/b = p\omega/(eE_0)$.

of induced tunneling, which extends the previously observed effect of coherent destruction of tunnelling.

We have also proposed using graphene electrodes for coherent control of electric transport via molecular junctions. The approach is based on the excitation of dressed states of the doped graphene with electric field, having used unique properties of the graphene. We have calculated a semiclassical wave function of a doped graphene under the action of EM excitation and the current through a molecular junction with graphene electrodes using nonequilibrium Green functions. We have shown that using graphene electrodes can essentially enhance currents evaluated at side-band energies $\sim n\hbar\omega$ in molecular nanojunctions that is related to the modification of the graphene gapless spectrum under the action of external EM field. We have calculated the corresponding quasienergy spectrum that is accompanied with opening the gap induced by intraband excitations.

ACKNOWLEDGMENTS

I acknowledge support by the US-Israel Binational Science Foundation and the Northwestern-Tel Aviv University Exchange Program.

REFERENCES

1. S. Kohler, J. Lehmann, and P. Hanggi, *Phys. Reports* **406**, 379–443 (2005).
2. F. Chen, and N. J. Tao, *Accounts of Chemical Research* **42**, 429 (2009).
3. B. D. Fainberg, M. Sukharev, T.-H. Park, and M. Galperin, *Phys. Rev. B* **83**, 205425 (2011).
4. M. G. Reuter, M. Sukharev, and T. Seideman, *Phys. Rev. Lett.* **101**, 208303 (2008).
5. U. Kleinekathofer, G. Li, S. Welack, and M. Schreiber, *Europhys. Letters* **79**, 27006 (2007).
6. B. D. Fainberg, M. Jouravlev, and A. Nitzan, *Phys. Rev. B* **76**, 245329 (2007).
7. A. Zrenner, E. Beham, S. Stufler, F. Findeis, M. Bichler, and G. Abstreiter, *Nature* **418**, 612–614 (2002).
8. B. Fainberg, and A. Nitzan, *Physica Status Solidi A* **206**, 948–951 (2009), [arXiv: 0808.1759 (cond-mat.mes-hall)].
9. G. Platero, and R. Aguado, *Phys. Reports* **395**, 1–157 (2004).
10. A. H. L. Dayem, and R. J. Martin, *Phys. Rev. Lett.* **8**, 246 (1962).
11. P. K. Tien, and J. P. Gordon, *Phys. Rev.* **129**, 647–651 (1963).
12. A. H. C. Neto, F. Guinea, N. M. R. Peres, K. S. Novoselov, and A. K. Geim, *Rev. Mod. Phys.* **81**, 109–162 (2009).
13. S. V. Syzranov, M. V. Fistul, and K. B. Efetov, *Phys. Rev. B* **78**, 045407 (2008).
14. X. Zheng, S.-H. Ke, and W. Yang, *J. of Chem. Phys* **132**, 114703 (2010).
15. S. A. Mikhailov, *Europhys. Letters* **79**, 27002 (2007).
16. B. D. Fainberg, and T. Seideman, *Chem. Phys. Lett.* **576**, 1–9 (2013), [Frontiers Article].
17. B. Fainberg, and T. Seideman, *Phys. Status Solidi A* **209**, 2433–2436 (2012).
18. B. D. Fainberg, *Opt. Spectrosc.* **41**, 228–231 (1976), [Opt. Spektrosk., vol. 41, 397, 1976].
19. V. L. Bogdanov, and B. D. Fainberg, *Opt. Spectrosc.* **41**, 472–474 (1976), [Opt. Spektrosk., vol. 41, n. 5, p. 799-802, 1976].
20. B. D. Fainberg, *Opt. Spectrosc.* **41**, 558–562 (1976), [Opt. Spektrosk., vol. 41, n. 6, p.944-951, 1976].
21. B. D. Fainberg, V. A. Gorbunov, and S. H. Lin, *Chem. Phys.* **307**, 77–90 (2004).
22. S. Welack, M. Schreiber, and U. Kleinekathofer, *J. Chem. Phys.* **124**, 044712 (2006).
23. G. Li, B. D. Fainberg, A. Nitzan, S. Kohler, and P. Hanggi, *Phys. Rev. B* **81**, 165310 (2010).
24. F. Grossmann, T. Dittrich, P. Jung, and P. Hanggi, *Phys. Rev. Lett.* **67**, 516–519 (1991).
25. B. D. Fainberg, *Phys. Rev. B* **88**, 245435 (2013).
26. W. Pauli, *Helv. Phys. Acta* **5**, 179 (1932).
27. A. I. Akhiezer, and V. B. Berestetskii, *Quantum electrodynamics*, Nauka, Moskow, 1969, in Russian.
28. H. Haug, and A. P. Jauho, *Quantum Kinetics in Transportand Optics of Semiconductors*, Springer, Berlin, 1996.
29. M. Abramowitz, and I. Stegun, *Handbook on Mathematical Functions*, Dover, New York, 1964.
30. G. Li, M. S. Shishodia, B. D. Fainberg, B. Apter, M. Oren, A. Nitzan, and M. Ratner, *Nano Letters* **12**, 2228–2232 (2012).
31. T. Oka, and H. Aoki, *Phys. Rev. B* **79**, 081406 (2009).